

Direct Measurement of the Forbidden $2^3S_1 \rightarrow 3^3S_1$ Atomic Transition in Helium

K. F. Thomas¹, J. A. Ross, B. M. Henson, D. K. Shin¹, K. G. H. Baldwin, S. S. Hodgman, and A. G. Truscott^{1*}
Laser Physics Centre, Research School of Physics, The Australian National University, Canberra, ACT 2601, Australia

 (Received 17 February 2020; accepted 12 June 2020; published 1 July 2020)

We present the detection of the highly forbidden $2^3S_1 \rightarrow 3^3S_1$ atomic transition in helium, the weakest transition observed in any neutral atom. Our measurements of the transition frequency, upper state lifetime, and transition strength agree well with published theoretical values and can lead to tests of both QED contributions and different QED frameworks. To measure such a weak transition, we develop two methods using ultracold metastable (2^3S_1) helium atoms: low background direct detection of excited then decayed atoms for sensitive measurement of the transition frequency and lifetime, and a pulsed atom laser heating measurement for determining the transition strength. These methods could possibly be applied to other atoms, providing new tools in the search for ultraweak transitions and precision metrology.

DOI: 10.1103/PhysRevLett.125.013002

The field of precision spectroscopy has made many foundational contributions to modern physics [1–4], in particular through the development of quantum electrodynamics (QED) theory. However, despite QED being one of the most rigorously tested theories in physics, there are still unknown factors and parameters, as shown by the recent “proton radius puzzle” that required a reassessment of the proton radius [5–8]. This leads to an imperative to test QED at the highest precision using independent methods in order to better understand its limitations. Advances in laser technology have enabled the detection of an increasingly wide array of atomic transitions, including extremely weak atomic spectral lines from so-called forbidden transitions, which within a given approximation, e.g., the electric dipole approximation, strictly cannot occur. However, in reality such transitions do occur but at extremely low rates. The strength of an atomic transition is characterized by the Einstein A coefficient (the transition rate), which is challenging to calculate or measure accurately. However, in some atomic systems the Einstein A coefficient has a significant and potentially measurable contribution from QED effects [9]. Hence, measurements of the Einstein A coefficient can provide a test of QED, completely independent of, for example, the measurement of atomic energy intervals. Note that while there are other means of measuring transition rate information in atomic systems in order to test QED, such as the tune-out frequency (the frequency at which the atomic polarizability vanishes [10–12]), they often relate to the ratio of strong transition rates between multiple states. Thus, these techniques do not measure the isolated strength of a single transition, which can provide additional insights and be important for specific applications, nor are they useful for measuring or constraining ultraweak transitions [13].

A favored test bed of QED models is the helium atom, where the two-electron structure is simple enough that

theoretical calculations of many parameters can be determined to great precision. Decades of work on ^3He and ^4He systems have led to many advances, such as an improved measurement of the ground state Lamb shift [14,15], the fine structure constant [16,17], and both the alpha and helion particle charge radius [18,19]. There have also been a number of recent advancements in precision spectroscopy of forbidden transitions in the helium atom. For instance, the $2^3S_1 \rightarrow 2^1P_1$ transition (see Fig. 1), which is forbidden as it violates spin conservation and has a predicted Einstein A value of $A = 1.4432 \text{ s}^{-1}$ [20], was first observed by Notermans *et al.* to a precision of 0.5 MHz [21].

Furthermore, a second extremely weak helium transition of interest is the singlet to triplet ground state transition of metastable helium (He^*) $2^3S_1 \rightarrow 2^1S_0$ (see Fig. 1), which is

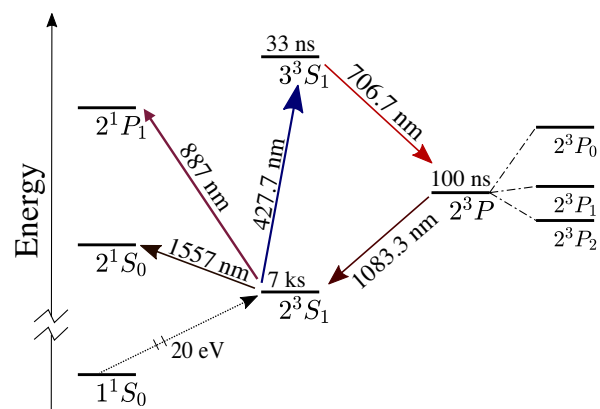


FIG. 1. Partial atomic level scheme for helium. Level splittings are not to scale. The transition of interest, $2^3S_1 \rightarrow 3^3S_1$, is at 427.7 nm (blue arrow), along with the dominant decay path from the 3^3S_1 state (706.7 nm, red arrow). Relevant excited state lifetimes and transition wavelengths are also indicated.

doubly forbidden, as it links a triplet to a singlet state, and $\Delta l = 0$. This transition has a predicted Einstein A coefficient ranging from $A = 6.1 \times 10^{-8} \text{ s}^{-1}$ [22] to $A = 1.5 \times 10^{-7} \text{ s}^{-1}$ [23], but the transition rate is yet to be measured. An experimental measurement of the transition frequency was carried out by van Rooij *et al.* to a precision of 2 kHz for both ^3He and ^4He [24]. Subsequent measurements by Rengelink *et al.* improved the precision to 0.2 kHz by using a magic wavelength trap [18], providing a new test of QED and nuclear structure calculations, including a determination of the nuclear charge radius. Of further note are the frequency measurements of seven of the transitions between the 2^3S and 2^3P hyperfine manifolds in ^3He by Cancio Pastor *et al.* to the order of 1 kHz [19]. This provided a value of the difference of the squared nuclear charge radii of ^3He and ^4He , which differed by 4σ from that derived by van Rooij *et al.*, exemplifying the need to perform different types of experiments to properly constrain QED theory.

Another transition in helium that until now has not been detected experimentally is the strongly forbidden $2^3S_1 \rightarrow 3^3S_1$ transition (see Fig. 1), for which $\Delta l = 0$, and it is hence electric dipole forbidden. It is excited via the magnetic dipole interaction using light with a predicted wavelength of $\sim 427.7 \text{ nm}$ [25]. There are unresolved conflicting theoretical predictions for the Einstein A coefficient of this transition. Derevianko *et al.* predict $A = 1.17 \times 10^{-8} \text{ s}^{-1}$ [26], while a calculation by Łach *et al.* gives $A = 6.48 \times 10^{-9} \text{ s}^{-1}$ [27], which states in reference to the differing values “*This discrepancy does not have experimental impact since this rate is too small ... to be measured*” [27]. An accurate measurement of the Einstein A coefficient for this transition would provide insight into the validity and limitations of the different approaches within QED theory. These calculations also indicate that this transition rate would be the weakest ever measured in a neutral atom and only slightly stronger than the weakest measured transition rate in an ion: the electric-octupole transition in $^{172}\text{Yb}^+$, which is the longest lived at 8.4 years, i.e., $A = 3.8 \times 10^{-9} \text{ s}^{-1}$ (theory [28]), or 10_{-4}^{+7} years, equivalently $A = 3_{-1}^{+2} \times 10^{-9} \text{ s}^{-1}$ (experiment [29]).

In this work, we present the first detection of the $2^3S_1 \rightarrow 3^3S_1$ transition in ^4He . We develop two novel techniques for the measurement of ultraweak transitions and use them to determine the transition frequency, Einstein A coefficient, and excited state lifetime. The first method uses a Bose-Einstein condensate (BEC) and directly detects atoms that absorb a photon and escape a shallow trap. While this method is highly sensitive and is ideal for the determination of the transition frequency and linewidth, the uncertainty in the collection efficiency necessitates an independent approach for determining the Einstein A coefficient. To this end, we developed a second method, which measures the heating rate of a trapped thermal cloud due to the

absorption and subsequent reemission of photons from a probe beam. From this the Einstein A coefficient can be extracted. While detection of an excitation via heating due to a photon recoil has been used for great precision and sensitivity in ion spectroscopy [29–32], this is the first time such a technique has been used in a neutral atom system. A similar technique could possibly be used to search for other weak transitions that have applications in astronomy and state-of-the-art technologies, such as atomic clocks [33].

To measure the transition frequency and linewidth, we start with a BEC of $\sim 10^6 \text{ He}^*$ atoms trapped in the long-lived 2^3S_1 excited state [34], prepared via a combination of laser and evaporative cooling in a magnetic biplanar quadrupole Ioffe trap [35]. The atoms are prepared in the $m_J = +1$ magnetic substate, as this is the only magnetically trapped state [35]. The atoms are detected after falling onto an 80 mm diameter microchannel plate and delay line detector (DLD) [36] (see remark [33] for extensions to other atoms), located approximately 850 mm below the trap center (Fig. 2).

To address the $2^3S_1 \rightarrow 3^3S_1$ transition, we illuminate the atoms with a probe beam from a laser and doubling cavity that is tuneable around 427.7 nm [37]. The frequency of the laser was stabilized using a feedback loop to a wave meter with 2 MHz absolute accuracy, which was periodically calibrated to a known cesium crossover transition (see Supplemental Material [37] for further detail). After passing through an optical fiber, the probe beam is focused and aligned along the weak axis of the trap (see Fig. 2 for diagram of experimental setup). We then perform differential measurements between the laser applied and a reference shot with the laser blocked.

The transition is detected by directly measuring small numbers, on the order of 10^2 , of atoms that absorb the probe laser light during a 25 s exposure time. When the wavelength of a σ^- polarized probe laser beam is resonant with the $2^3S_1 \rightarrow 3^3S_1$ transition, the 427.7 nm photon excites the atom from the 2^3S_1 , $m_J = +1$ state to the 3^3S_1 , $m_J = 0$ state and the atom receives a momentum recoil. The vast majority of these excited atoms then decay within $\sim 30 \text{ ns}$, emitting a photon at 706.7 nm to one of the

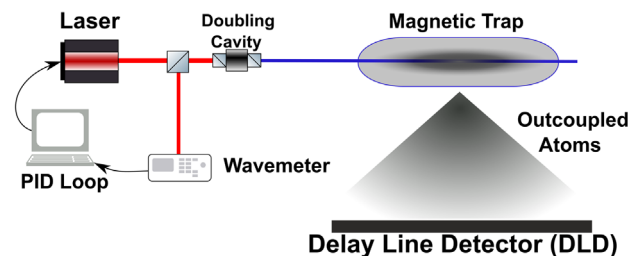


FIG. 2. Diagram of the experimental setup. A BEC is produced and then held in a magnetic trap. The laser light is focused onto the atoms in the trap and when an atom absorbs one of the photons it will most likely leave the trap, with some high probability of it landing on the detector.

$2^3P_{0,1,2}$ states, and then within ~ 100 ns decay via the 1083 nm transitions to the 2^3S_1 state (see Fig. 1). This is because all other transitions from 3^3S_1 and the $2^3P_{0,1,2}$ states are forbidden: hence, fewer than 1 in 10^4 atoms will decay to non- 2^3S_1 states [63,64].

Atoms will hence on average end up distributed among the magnetic sublevels $m_J = (-1, 0, 1)$ of the 2^3S_1 state with a fractional population of (24%, 52%, 24%) based on the relevant transition Clebsch–Gordan coefficients. The 76% of atoms that decay to the untrapped 2^3S_1 , $m_J = 0$ or -1 states leave the trap immediately and fall under the influence of gravity onto the DLD, with the chance that they will collide with other atoms while leaving the BEC [37].

The remaining 24% of excited atoms that have decayed to the 2^3S_1 , $m_J = +1$ state will be retrapped.

After the probe beam is switched off, the remaining atoms in the magnetic trap are outcoupled with pulses of broadband rf radiation. This transfers all atoms from the trap into a coherent beam of atoms, known as an atom laser [36,65], allowing the total number of remaining atoms in the trap to be measured, while avoiding detector saturation. The ratio of excited and lost atoms to remaining atoms can hence be determined, which is less sensitive to total BEC number fluctuations from shot to shot.

For each laser wavelength, ~ 215 shots are taken with the probe beam applied and ~ 50 with it blocked as a reference, from which the normalized excitation probability per photon per unit time [37] is extracted. The excited fractions for a range of frequencies around the transition are shown in Fig. 3. At resonance, we measure a peak signal corresponding to 0.34% of the total atoms excited per $\sim 10^{18}$ applied photons (for details on the beam shape and power in relation to the atom sample, see Supplemental Material [37]). Note that the signal in Fig. 3 decays to a negative value far from the transition. We speculate that this is due to the off-resonant repulsive dipole potential of the probe beam on the atoms, which causes a deflection of atoms such that they miss the detector, compared to the reference case. While this effect is measurable, it has a negligible effect on the line shape compared to the other sources of error [37].

The center of the corresponding Lorentzian fit gives a measured transition frequency of $f_{0,d} = 700\,939\,271.64(8)$ MHz, with subscript d referring to the direct detection method and with only the statistical uncertainty shown. After applying relevant systematic corrections (as listed with the full error budget in Table I), this yields a final value of $f_{0,d}^{\text{shifted}} = 700\,939\,271(5)$ MHz. This agrees very well with the most recent published value in the literature of $700\,939\,269(8)$ MHz [25], with our uncertainty smaller than that of theory. The Lorentzian width of the peak, derived from the Voigt fit (see Fig. 3), also allows the state lifetime of the 3^3S_1 state to be determined. We estimate an excited state

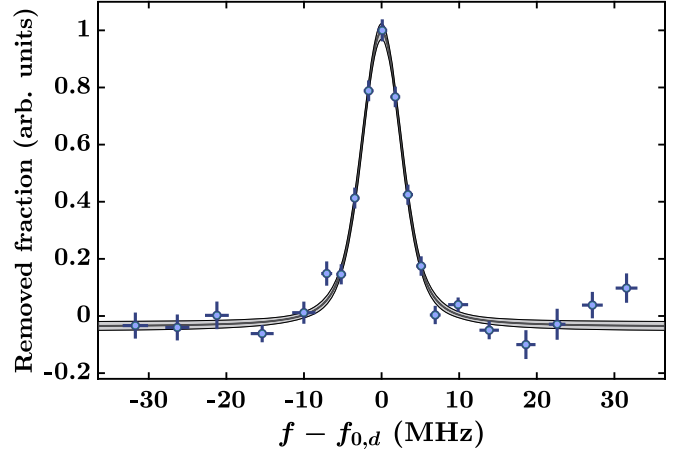


FIG. 3. The normalized excited fraction as a function of applied laser frequency (relative to the fitted centered frequency $f_{0,d} = 700\,939\,271.64(8)$ MHz where quoted error is purely statistical). Vertical and horizontal bars indicate the uncertainty in their respective axis [66]. Data has been binned for viewing, where the width of the bin used to calculate each point is varied to compensate for the varying density of sample points. The black line is a Voigt fit to the data, with the gray shaded region indicating the confidence interval. The parameters of the fit are $\sigma = 1.9(4)$ MHz (standard deviation of the Gaussian component) and $\gamma = 3.2(10)$ MHz (scale parameter of the Lorentzian component), corresponding to an excited state lifetime of 50(20) ns. The peak signal represents an excited fraction of 0.34% for a total energy of applied photons of 0.65 J.

lifetime of $\tau = 50(20)$ ns, which compares well to the theoretical value of 35.9(2) ns (see Supplemental Material [37]). We also find that the sensitivity of this method is such that an Einstein A value of $\approx 7 \times 10^{-11} \text{ s}^{-1}$ could be observed with a SNR of unity given one day of interrogation [37].

TABLE I. Systematic shifts, corrections, and uncertainties to measured frequency values from the direct detection method $f_{0,d}$ and the heating method $f_{0,h}$. Note that uncertainties are added in quadrature.

Value	Systematic Freq Shift (MHz)		Unc (MHz)	
	$f_{0,d}$	$f_{0,h}$	$f_{0,d}$	$f_{0,h}$
Zeeman shift	-1.715		0.003	
ac Stark shift	6.9	5.9	1.5	1.6
dc Stark shift	$< 10^{-6}$...	
Mean field shift	< 0.01		...	
Recoil shift	0.273		< 0.001	
Cesium cell offset				
-ac Stark shift	-1.9		0.4	
-Pressure shift	< 0.006		...	
Wave meter	-3.0		4.1	
Statistical	...		0.08	0.6
Total	0.6	-0.4	4.4	4.5

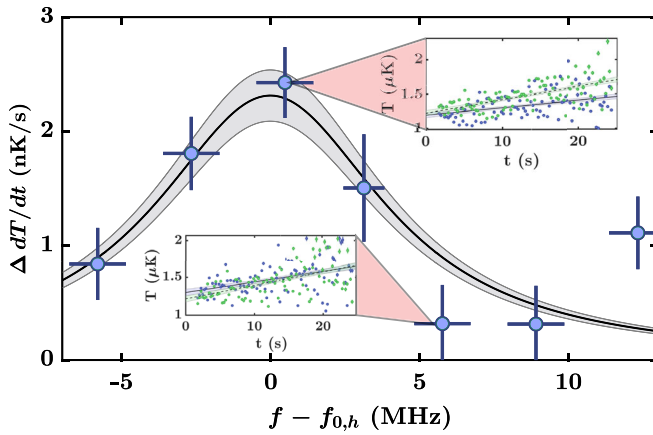


FIG. 4. Increase in heating rate as a function of applied laser frequency, relative to fitted frequency center $f_{0,h} = 700\,939\,270.9(6)$ MHz, with quoted error purely statistical. Data has been binned in frequency for clarity, with vertical and horizontal bars indicating uncertainty in the respective axis [66]. The solid black line represents a Voigt fit with $\sigma = 1.6(9)$ MHz, and $\gamma = 4(3)$ MHz. The insets show a comparison of heating rates at the respective frequencies, with the dashed (green) line indicating a run with the laser light applied and the solid (blue) line indicating a reference run.

To measure the transition strength, we employ a different experimental technique that determines the heating of the cloud induced by the photon recoil of absorbed and emitted photons from the probe beam. The thermal cloud has an initial temperature of order $1\ \mu\text{K}$. We use a minimally destructive spectrally broad rf pulse to remove $\sim 2\%$ of the atoms from the trap. The pulses are approximately $20\ \mu\text{s}$ in length and hence have a Fourier width of $\sim 300\ \text{kHz}$ [36], which ensures uniform outcoupling throughout the trap. The time-of-flight profile recorded on the DLD in the far field will represent the momentum profile of the trapped atoms [67]. As the temperature of the atoms is significantly above the condensation temperature, $T_c \sim 150\ \text{nK}$, the temperature was found by fitting each profile with a Boltzmann distribution (see Supplemental Material [37]). By repeatedly outcoupling small numbers of atoms (the full sequence uses 95 pulses each spaced 240 ms apart), the temperature of the trapped thermal cloud can be estimated as a function of time and thus a heating rate determined. Comparison of the measured heating rate when the probe beam is present to when it is blocked allows an estimate of the heating rate due to the probe beam. The difference in the heating rates between probe and reference is shown in Fig. 4 as a function of laser frequency, which gives a fitted peak frequency for this method of $f_{0,h}^{\text{shifted}} = 700\,939\,270.9(6)$ MHz (with subscript h referring to the heating method and with the statistical uncertainty shown). After applying appropriate systematic frequency shifts (see Table I in [37]), the final value for the transition frequency is $f_{0,h} = 700\,939\,271(5)$ MHz, and the excited state

TABLE II. Summary table of experimentally measured values, including all systematic corrections, for the $2^3S_1 \rightarrow 3^3S_1$ transition in Helium, with the most recent theoretical calculations for comparison.

Method	Center Freq (MHz)	3^3S_1 State Lifetime (ns)	Einstein A Coeff ($10^{-9}\ \text{s}^{-1}$)
Direct	700939271(5)	50(20)	...
Heating	700939271(5)	40(30)	7(4)
Theory	700939269(8)[25]	35.9(2)[37]	6.48[27], 11.7[26]

lifetime is $40(30)$ ns. Both agree within uncertainty with the values measured by the direct detection method.

We calculate the Einstein A coefficient from the measured heating rate and the heat capacity of a harmonically trapped Bose gas [37]. The resultant value is $A = 7(4) \times 10^{-9}\ \text{s}^{-1}$ compared to the most recent theoretical value of $A = 6.48 \times 10^{-9}\ \text{s}^{-1}$ [27].

Our results for the transition frequency using both methods compare well with the most recent theoretical value in the literature (see Table II), and our experimental uncertainty is comparable to that of the current QED theory calculation. A further consequence of our measurement of the $2^3S_1 \rightarrow 3^3S_1$ transition wavelength is that it constrains the $2^3P_1 \rightarrow 3^3S_1$ transition frequency to be $424202774(5)$ MHz, using the extremely accurately measured $2^3S_1 \rightarrow 2^3P_1$ transition frequency [68]. Further, the experimental Einstein A coefficient also agrees within error with both of the most recent theoretical published values [26,27], although it is not sufficiently sensitive to resolve the difference between them. Nonetheless, the measurement of transition strengths is important as an alternative test for QED, as there are few techniques that can be compared to energy level measurements, and thus further investigation is warranted.

In conclusion, we have demonstrated a novel sensitive method for measuring and characterizing spectroscopic transitions in helium that could in principle be extended to other metastable atoms, particularly those that are used in ultracold gas experiments [69]. This has allowed us to detect the weakest transition ever observed in a neutral atom. The techniques are based upon momentum detection of atoms, separating them from most other techniques in the literature that are usually based on measuring change in irradiance. While our method agrees within experimental uncertainty with theory, by increasing the accuracy of the laser wavelength measurement (e.g., via incorporating a frequency comb), we could reach a level of accuracy of < 1 MHz, which would provide a challenge to improve state-of-the-art theoretical predictions. Furthermore, by conducting similar measurements on ^3He , isotope shifts could also be compared as a further test of QED predictions.

The authors would like to thank G. W. F. Drake, G. Łach, and K. Pachucki for helpful discussions, and C. J. Vale and S. Hoinka for the loan of the laser. This work was supported through Australian Research Council (ARC) Discovery Project Grants No. DP160102337 and DP180101093, as well as Linkage Project No. LE180100142. K. F. T. and D. K. S. are supported by Australian Government Research Training Program (RTP) scholarships. S. S. H. is supported by ARC Discovery Early Career Researcher Award No. DE150100315.

*Corresponding author.

andrew.truscott@anu.edu.au

- [1] A. H. Compton, A quantum theory of the scattering of X-rays by light elements, *Phys. Rev.* **21**, 483 (1923).
- [2] G. Landsberg and L. Mandelstam, A novel effect of light scattering in crystals, *Naturwissenschaften* **16**, 557 (1928).
- [3] C. V. Raman and K. S. Krishnan, The optical analogue of the Compton effect, *Nature (London)* **121**, 711 (1928).
- [4] W. E. Lamb and R. C. Retherford, Fine structure of the hydrogen atom by a microwave method, *Phys. Rev.* **72**, 241 (1947).
- [5] R. Pohl, A. Antognini, F. Nez, F. D. Amaro *et al.*, The size of the proton, *Nature (London)* **466**, 213 (2010).
- [6] A. Antognini, F. Nez, K. Schuhmann, F. D. Amaro *et al.*, Proton structure from the measurement of 2S-2P transition frequencies of muonic hydrogen, *Science* **339**, 417 (2013).
- [7] N. Bezginov, T. Valdez, M. Horbatsch, A. Marsman, A. C. Vutha, and E. A. Hessels, A measurement of the atomic hydrogen lamb shift and the proton charge radius, *Science* **365**, 1007 (2019).
- [8] W. Xiong, A. Gasparian, H. Gao *et al.*, A small proton charge radius from an electron-proton scattering experiment, *Nature (London)* **575**, 147 (2019).
- [9] O. Y. Andreev, L. N. Labzowsky, and G. Plunien, QED calculation of transition probabilities in two-electron ions, *Phys. Rev. A* **79**, 032515 (2009).
- [10] L. J. LeBlanc and J. H. Thywissen, Species-specific optical lattices, *Phys. Rev. A* **75**, 053612 (2007).
- [11] B. M. Henson, R. I. Khakimov, R. G. Dall, K. G. H. Baldwin, L.-Y. Tang, and A. G. Truscott, Precision Measurement for Metastable Helium Atoms of the 413 nm Tune-Out Wavelength at Which the Atomic Polarizability Vanishes, *Phys. Rev. Lett.* **115**, 043004 (2015).
- [12] Y.-H. Zhang, F.-F. Wu, P.-P. Zhang, L.-Y. Tang, J.-Y. Zhang, K. G. H. Baldwin, and T.-Y. Shi, QED and relativistic nuclear recoil corrections to the 413-nm tune-out wavelength for the 2^3S_1 state of helium, *Phys. Rev. A* **99**, 040502 (R) (2019).
- [13] J. Pickering, R. Blackwell-Whitehead, A. Thorne, M. Ruffoni, and C. Holmes, Laboratory measurements of oscillator strengths and their astrophysical applications, *Can. J. Phys.* **89**, 387 (2011).
- [14] D. Z. Kandula, C. Gohle, T. J. Pinkert, W. Ubachs, and K. S. Eikema, Extreme Ultraviolet Frequency Comb Metrology, *Phys. Rev. Lett.* **105**, 063001 (2010).
- [15] S. D. Bergeson, A. Balakrishnan, K. G. H. Baldwin, T. B. Lucatorto, J. P. Marangos, T. J. McIlrath, T. R. O'Brian, S. L. Rolston, C. J. Sansonetti, J. Wen, N. Westbrook, C. H. Cheng, and E. E. Eyler, Measurement of the He Ground State Lamb Shift Via the Two-Photon $1^1S - 2^1S$ Transition, *Phys. Rev. Lett.* **80**, 3475 (1998).
- [16] M. Smiciklas and D. Shiner, Determination of the Fine Structure Constant Using Helium Fine Structure, *Phys. Rev. Lett.* **105**, 123001 (2010).
- [17] K. Kato, T. D. G. Skinner, and E. A. Hessels, Ultrahigh-Precision Measurement of the $n = 2$ Triplet p Fine Structure of Atomic Helium Using Frequency-Offset Separated Oscillatory Fields, *Phys. Rev. Lett.* **121**, 143002 (2018).
- [18] R. J. Rengelink, Y. van der Werf, R. P. M. J. W. Notermans, R. Jannin, K. S. E. Eikema, M. D. Hoogerland, and W. Vassen, Precision spectroscopy of helium in a magic wavelength optical dipole trap, *Nat. Phys.* **14**, 1132 (2018).
- [19] P. Cancio Pastor, L. Consolino, G. Giusfredi, P. De Natale, M. Inguscio, V. A. Yerokhin, and K. Pachucki, Frequency Metrology of Helium Around 1083 nm and Determination of the Nuclear Charge Radius, *Phys. Rev. Lett.* **108**, 143001 (2012).
- [20] G. W. F. Drake and D. C. Morton, A multiplet table for neutral helium ($^4\text{He I}$) with transition rates, *Astrophys. J. Suppl. Ser.* **170**, 251 (2007).
- [21] R. P. M. J. W. Notermans and W. Vassen, High-Precision Spectroscopy of the Forbidden $2^3S_1 \rightarrow 2^1P_1$ Transition in Quantum Degenerate Metastable Helium, *Phys. Rev. Lett.* **112**, 253002 (2014).
- [22] E. V. Baklanov and A. V. Denisov, Probability of the $2^1S_0 - 2^3S_1$ forbidden transition in the helium atom, *Quantum Electron.* **27**, 463 (1997).
- [23] C. D. Lin, W. R. Johnson, and A. Dalgarno, Radiative decays of the $n = 2$ states of He-like ions, *Phys. Rev. A* **15**, 154 (1977).
- [24] R. van Rooij, J. S. Borbely, J. Simonet, M. D. Hoogerland, K. S. E. Eikema, R. A. Rozendaal, and W. Vassen, Frequency metrology in quantum degenerate helium: Direct measurement of the $2^3S_1 \rightarrow 2^1S_0$ transition, *Science* **333**, 196 (2011).
- [25] G. W. F. Drake, in *Springer Handbook of Atomic, Molecular, and Optical Physics* (Springer-Verlag, New York, 2006), pp. 199–219.
- [26] A. Derevianko, I. M. Savukov, W. R. Johnson, and D. R. Plante, Negative-energy contributions to transition amplitudes in heliumlike ions, *Phys. Rev. A* **58**, 4453 (1998).
- [27] G. Łach and K. Pachucki, Forbidden transitions in the helium atom, *Phys. Rev. A* **64**, 042510 (2001).
- [28] E. Biémont and P. Quinet, Theoretical Study of the $4f^{14}6s^2\ ^2S_{1/2} - -4f^{13}6s^2\ ^2F_{7/2}^0\ E3$ Transition in Yb II, *Phys. Rev. Lett.* **81**, 3345 (1998).
- [29] M. Roberts, P. Taylor, G. P. Barwood, P. Gill, H. A. Klein, and W. R. C. Rowley, Observation of an Electric Octupole Transition in a Single Ion, *Phys. Rev. Lett.* **78**, 1876 (1997).
- [30] Y. Wan, F. Gebert, J. B. Wübbena, N. Scharnhorst, S. Amairi, I. D. Leroux, B. Hemmerling, N. Lörch, K. Hammerer, and P. O. Schmidt, Precision spectroscopy by photon-recoil signal amplification, *Nat. Commun.* **5**, 3096 (2014).

- [31] F. Gebert, Y. Wan, F. Wolf, C.N. Angstmann, J.C. Berengut, and P.O. Schmidt, Precision Isotope Shift Measurements in Calcium Ions Using Quantum Logic Detection Schemes, *Phys. Rev. Lett.* **115**, 053003 (2015).
- [32] M. Guggemos, M. Guevara-Bertsch, D. Heinrich, O.A. Herrera-Sancho, Y. Colombe, R. Blatt, and C.F. Roos, Frequency measurement of the $^1S_0, f = 5/2 \leftrightarrow ^3P_1, f = 7/2$ transition of $^{27}\text{Al}^+$ via quantum logic spectroscopy with $^{40}\text{Ca}^+$, *New J. Phys.* **21**, 103003 (2019).
- [33] This detection method only works for atoms with a high internal energy, such as He^* atoms or other excited noble gases; for other atomic species lacking this property, one would have to use a different, though comparable, detection method such as absorption imaging or continuous light sheet detection.
- [34] S. S. Hodgman, R. G. Dall, L. J. Byron, K. G. H. Baldwin, S. J. Buckman, and A. G. Truscott, Metastable Helium: A New Determination of the Longest Atomic Excited-State Lifetime, *Phys. Rev. Lett.* **103**, 053002 (2009).
- [35] R. Dall and A. Truscott, Bose–Einstein condensation of metastable helium in a bi-planar quadrupole Ioffe configuration trap, *Opt. Commun.* **270**, 255 (2007).
- [36] A. G. Manning, S. S. Hodgman, R. G. Dall, M. T. Johnsson, and A. G. Truscott, The Hanbury Brown-Twiss effect in a pulsed atom laser, *Opt. Express* **18**, 18712 (2010).
- [37] See Supplemental Material at <http://link.aps.org/supplemental/10.1103/PhysRevLett.125.013002> for further details, which includes Refs. [38–62].
- [38] C. E. Tanner and C. Wieman, Precision measurement of the hyperfine structure of the ^{133}Cs $6P_{3/2}$ state, *Phys. Rev. A* **38**, 1616 (1988).
- [39] Technical Information Wavelengthmeter WS8-2, HighFinesse GmbH, 2019.
- [40] D. A. Kondratjev, I. L. Beigman, and L. A. Vainshtein, Static polarizabilities of helium and alkali atoms, and their isoelectronic ions, *J. Russ. Laser Res.* **31**, 294 (2010).
- [41] P. S. Julienne and F. H. Mies, Collisions of ultracold trapped atoms, *J. Opt. Soc. Am. B* **6**, 2257 (1989).
- [42] T. C. Killian, D. G. Fried, L. Willmann, D. Landhuis, S. C. Moss, T. J. Greytak, and D. Kleppner, Cold Collision Frequency Shift of the $1S - 2S$ Transition in Hydrogen, *Phys. Rev. Lett.* **81**, 3807 (1998).
- [43] S. Moal, M. Portier, J. Kim, J. Dugué, U. D. Rapol, M. Leduc, and C. Cohen-Tannoudji, Accurate Determination of the Scattering Length of Metastable Helium Atoms Using Dark Resonances Between Atoms and Exotic Molecules, *Phys. Rev. Lett.* **96**, 023203 (2006).
- [44] S. Seidelin, J. V. Gomes, R. Hoppeler, O. Sirjean, D. Boiron, A. Aspect, and C. I. Westbrook, Getting the Elastic Scattering Length by Observing Inelastic Collisions in Ultracold Metastable Helium Atoms, *Phys. Rev. Lett.* **93**, 090409 (2004).
- [45] G. F. Gribakin and V. V. Flambaum, Calculation of the scattering length in atomic collisions using the semiclassical approximation, *Phys. Rev. A* **48**, 546 (1993).
- [46] P. J. Leo, V. Venturi, I. B. Whittingham, and J. F. Babb, Ultracold collisions of metastable helium atoms, *Phys. Rev. A* **64**, 042710 (2001).
- [47] O. Talu and A. L. Myers, Reference potentials for adsorption of helium, argon, methane, and krypton in high-silica zeolites, *Colloids Surf. A* **187–188**, 83 (2001).
- [48] G. A. Pitz, D. E. Wertepny, and G. P. Perram, Pressure broadening and shift of the cesium D_1 transition by the noble gases and N_2 , H_2 , HD, D_2 , CH_4 , C_2H_6 , CF_4 , and ^3He , *Phys. Rev. A* **80**, 062718 (2009).
- [49] G. A. Pitz, C. D. Fox, and G. P. Perram, Pressure broadening and shift of the cesium D_2 transition by the noble gases and N_2 , H_2 , HD, D_2 , CH_4 , C_2H_6 , CF_4 , and ^3He with comparison to the D_1 transition, *Phys. Rev. A* **82**, 042502 (2010).
- [50] J. L. Margrave, Vapour pressure of the chemical elements (Nesmeyanov, A. N.), *J. Chem. Ed.* **41**, A590 (1964).
- [51] J. Mitroy and L.-Y. Tang, Tune-out wavelengths for metastable helium, *Phys. Rev. A* **88**, 052515 (2013).
- [52] V. Astapenko, *Polarization Bremsstrahlung on Atoms, Plasmas, Nanostructures and Solids* (Springer-Verlag, Berlin Heidelberg, 2013), Vol. 72.
- [53] F. L. Kien, P. Schneeweiss, and A. Rauschenbeutel, Dynamical polarizability of atoms in arbitrary light fields: General theory and application to cesium, *Eur. Phys. J. D* **67**, 92 (2013).
- [54] J. E. Stalnaker, D. Budker, S. J. Freedman, J. S. Guzman, S. M. Rochester, and V. V. Yashchuk, Dynamic stark effect and forbidden-transition spectral line shapes, *Phys. Rev. A* **73**, 043416 (2006).
- [55] C. N. Cohen-Tannoudji, The Autler-Townes effect revisited, in *Amazing Light* (Springer, New York, 1996), pp. 109–123.
- [56] P. Fendel, S. D. Bergeson, T. Udem, and T. W. Hänsch, Two-photon frequency comb spectroscopy of the 6s-8s transition in cesium, *Opt. Lett.* **32**, 701 (2007).
- [57] C.-M. Wu, T.-W. Liu, M.-H. Wu, R.-K. Lee, and W.-Y. Cheng, Absolute frequency of cesium 6S-8S 822 nm two-photon transition by a high-resolution scheme, *Opt. Lett.* **38**, 3186 (2013).
- [58] A. Kramida, Y. Ralchenko, J. Reader, and NIST ASD Team (2019), NIST Atomic Spectra Database (ver. 5.7.1), [Online]. Available: <https://physics.nist.gov/asd> [2019, November 10]. National Institute of Standards and Technology, Gaithersburg, MD.
- [59] M. C. E. Huber and R. J. Sandeman, The measurement of oscillator strengths, *Rep. Prog. Phys.* **49**, 397 (1986).
- [60] M. Ligare, Classical thermodynamics of particles in harmonic traps, *Am. J. Phys.* **78**, 815 (2010).
- [61] V. Krainov and B. M. Smirnov, *Atomic and Molecular Radiative Processes* (Springer International Publishing, Cham, 2019), Chap. 1.2.4, pp. 26–30.
- [62] H. J. Metcalf and P. Van der Straten, *Laser Cooling and Trapping* (Springer-Verlag, New York, 1999), Chap. 4, pp. 53–56.
- [63] R. G. Dall, K. G. H. Baldwin, L. J. Byron, and A. G. Truscott, Experimental Determination of the Helium $2^3P_1 - 1^1S_0$ Transition Rate, *Phys. Rev. Lett.* **100**, 023001 (2008).
- [64] S. S. Hodgman, R. G. Dall, K. G. H. Baldwin, and A. G. Truscott, Complete ground-state transition rates for the helium 2^3P manifold, *Phys. Rev. A* **80**, 044501 (2009).
- [65] B. M. Henson, X. Yue, S. S. Hodgman, D. K. Shin, L. A. Smirnov, E. A. Ostrovskaya, X. W. Guan, and A. G.

- Truscott, Bogoliubov-Cherenkov radiation in an atom laser, *Phys. Rev. A* **97**, 063601 (2018).
- [66] Vertical bars indicate standard error in signal of the respective sample, and horizontal bars are the quadrature sum of the standard error in frequency and the standard error of wave meter calibrations.
- [67] I. Yavin, M. Weel, A. Andreyuk, and A. Kumarakrishnan, A calculation of the time-of-flight distribution of trapped atoms, *Am. J. Phys.* **70**, 149 (2002).
- [68] X. Zheng, Y.R. Sun, J.-J. Chen, W. Jiang, K. Pachucki, and S.-M. Hu, Measurement of the Frequency of the $2^3S - 2^3P$ Transition of ^4He , *Phys. Rev. Lett.* **119**, 263002 (2017).
- [69] W. Vassen, C. Cohen-Tannoudji, M. Leduc, D. Boiron, C.I. Westbrook, A. Truscott, K. Baldwin, G. Birkl, P. Cancio, and M. Trippenbach, Cold and trapped metastable noble gases, *Rev. Mod. Phys.* **84**, 175 (2012).